atmosphere

MDPI

Article

Convective Core Dynamics and Sensitivity of Runoff Generation to Short-Duration Mediterranean Storms

Alberto Fortelli and Fabio Matano *

Istituto Scienze Marine, Consiglio Nazionale delle Ricerche, Calata Porta di Massa, Porto di Napoli, 80133 Napoli, Italy

* Correspondence: fabio.matano@cnr.it; Tel.: +39-081-5423834

Abstract

Short-duration rainfall extremes in Mediterranean regions are frequently produced by convective storms that concentrate most precipitation within narrow temporal windows. Standard Depth–Duration–Frequency (DDF) and Intensity–Duration–Frequency (IDF) approaches convert a selected duration and return period into constant-intensity design storms, neglecting the temporal structure that governs runoff generation in fast-responding catchments. This study quantifies the bias introduced by this simplification using long-term 10 min rainfall records and a duration-consistent event-selection procedure. Events lasting 30, 40, 50 and 60 min were extracted from local VAPI(Progetto Speciale per la Valutazione delle Piene in Italia) DDF relationships and converted into dimensionless temporal profiles; hydrological sensitivity, however, was evaluated only for the 30- and 40 min storms, as longer durations were included solely in the rainfall analysis. The 30- and 40 min profiles exhibit marked convective concentration, with the most intense 10 min interval contributing up to 41.8% and 31.7% of total rainfall. Controlled SWMM (Storm Water Management Model) 5.2 simulations on a conceptual 6-ha peri-urban catchment, performed within a non-predictive sensitivity experiment, show that variable-intensity storms tend to increase peak discharge and shorten time to peak compared with constant-intensity storms of identical depth. These results indicate that constant-intensity DDF/IDF storms may underestimate peak runoff for short durations, underscoring the importance of incorporating locally derived temporal rainfall profiles in Mediterranean environments characterized by increasingly irregularshort-duration convective rainfall.

Keywords: short-duration rainfall extremes; convective core dynamics; temporal rainfall structure; 10 min precipitation data; variable-intensity convective storms; runoff sensitivity; Mediterranean convective regimes

Check for updates

Academic Editors: Ioannis Pytharoulis, Stergios Kartsios and Flavio T. Couto

Received: 28 August 2026
Revised: 5 October 2026
Accepted: 7 October 2026
Published: 14 October 2026

Copyright: © 2026 by the authors. Licensee MDPI, Basel, Switzerland. This article is an open access article distributed under the terms and conditions of the Creative Commons Attribution (CC BY) license.

1. Introduction

Short-duration rainfall extremes are among the most impactful components of contemporary hydroclimatic risk, particularly in Mediterranean climates where convective systems dominate sub-hourly precipitation [1]. Recent regional analyses [2] show that flash-flood response in Mediterranean areas is highly sensitive to the internal temporal structure of convective rainfall. These storms typically produce intense rainfall over short durations and limited spatial footprints. Their strong temporal concentration can trigger flash floods, sewer surcharge, surface flooding, and rainfall-induced mass movements within very short response times. Their relevance is increasing as the climate continues to warm, with observational and modeling studies consistently showing that sub-hourly and

hourly extremes intensify with atmospheric warming and are closely linked to convective processes [3–6]. Additional evidence indicates that short-duration extremes may intensify at rates exceeding Clausius–Clapeyron expectations, especially for hourly precipitation [7], highlighting their growing relevance under warming. These considerations provide physical context only; the present study does not perform any trend analysis nor infer climatic evolution from the rainfall dataset.

Convection-permitting modeling further confirms that high-resolution simulations substantially improve the representation of short-duration rainfall extremes [8]. Organized convective systems are also expected to intensify under warming, with implications for short-duration extremes in mid-latitude regions [9]. In Mediterranean environments, rainfall timing and temporal concentration are further modulated by coastal, urban, and orographic gradients, making high-resolution analyses essential for reliable hydrological and ground-level impact assessment [7].

In hydraulic and urban drainage engineering, Intensity–Duration–Frequency (IDF) and Depth–Duration–Frequency (DDF) curves provide the relationship between rainfall intensity or depth, event duration, and return period. Although indispensable for selecting design depths, the rainfall event derived from these curves is an idealization: in most practical applications, the selected depth is uniformly distributed over the duration, implicitly assuming constant intensity. Real convective storms rarely follow this pattern. Instead, rainfall is commonly concentrated in one or two short intervals, separated by lower-intensity phases and often confined to narrow spatial domains. This spatio-temporal variability may lead to underestimation of convective extremes when relying on standard gauge networks, with point-scale extremes potentially underestimated by up to 20% [7].

The hydrological implications are particularly relevant for small urban catchments, where response time may be comparable to the duration of the rainfall core [10]. This sensitivity is consistent with previous findings showing that urban hydrological response is strongly influenced by rainfall variability at fine temporal scales [11]. Previous studies show that design-storm selection, rainfall duration, peak position, and hyetograph shape can materially affect simulated flow rates, flood depths, and drainage-system robustness [12–15]. In this study, the modeling component is used exclusively as a controlled sensitivity experiment rather than as a predictive hydrological simulation. Despite this evidence, many operational procedures still rely on constant-intensity storms or on generic synthetic patterns. Common examples include Chicago, Huff, alternating-block, and average-variability approaches, which may not reflect local sub-hourly rainfall dynamics when applied without calibration [16,17]. Recent analyses further show that these traditional schemes often fail to reproduce the temporal concentration of real convective events, leading to biased hydrological estimates in urban catchments [18]. This issue is especially relevant for drainage systems in Mediterranean cities, where short-duration events dominate system response and where recent changes in rainfall regimes at fine temporal and spatial scales further increase the need for high-resolution analyses [19].

The objective of this study is to quantify the internal temporal concentration of 30–60 min rainfall events in the Naples metropolitan area and to evaluate, in a controlled SWMM experiment, how constant and variable-intensity storms of equal volume affect runoff response for the 30 and 40 min durations. From this point onward, we adopt the abbreviated form “xx-min”, which is used consistently throughout the manuscript.

Identifying and isolating significant rainfall events within continuous time series remains a well-known challenge in hydrological analysis. The Minimum Inter-Event Time (MIET) criterion is widely used, but no single extraction method is universally optimal, particularly when the aim is to isolate short convective cores rather than entire multi-phase storm systems [20]. MIET-based approaches are sensitive to temporal resolution,

which may hinder the identification of short convective bursts [21]. High-resolution event identification methods have been proposed to better isolate convective cores embedded within multi-phase storms [22].

In this study, we adopt a site-specific extraction procedure based on (a) thresholds derived from local DDF curves and (b) checks on the internal structure of rainfall sub-events embedded within larger storm sequences. The procedure also limits the multiple use of the same 10 min rainfall value across overlapping windows, preventing artificial inflation of event counts and ensuring that each event reflects a physically distinct convective core.

2. Materials and Methods

2.1. Rainfall Dataset and Geographic Context

The study area is located in the central–southern Mediterranean region, along the western coast of the Italian peninsula, in a central position within the Mediterranean basin (Figure 1). According to the Köppen–Trewartha climate classification [23], the area is characterized by a Mediterranean climate with dry summers and wet winters.

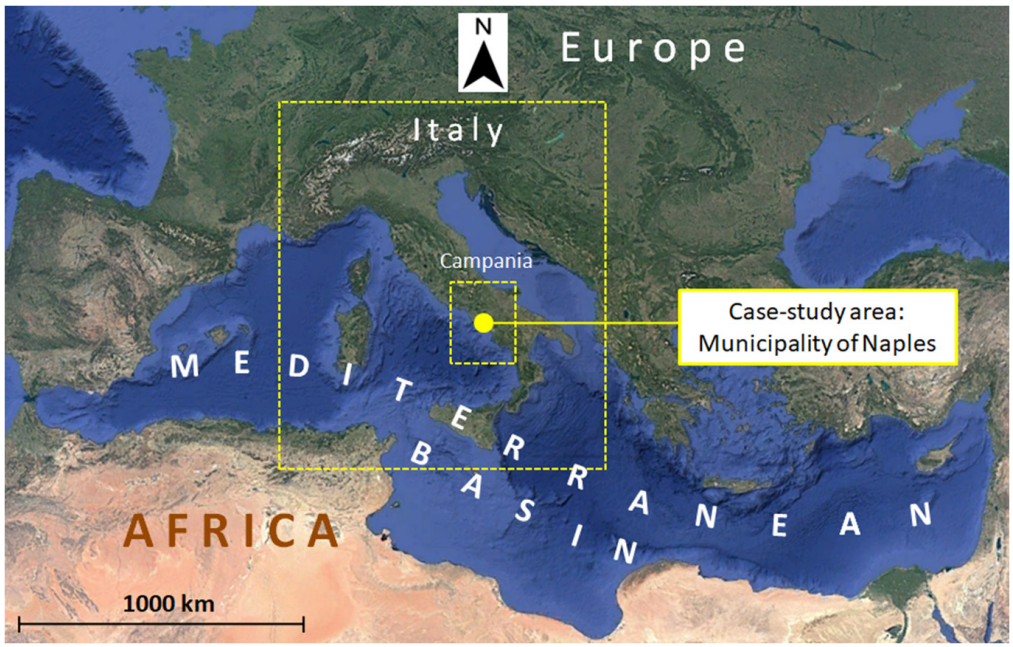

Figure 1. Geographical location of the Municipality of Naples within the Campania region and the broader Mediterranean Basin, identifying the spatial context of the rainfall dataset used to analyze sub-hourly convective events.

This climatic setting favors short, high-intensity convective storms during the transitional season from summer to autumn and warm-period instability episodes, making the region particularly prone to sub-hourly rainfall extremes [24]. Mediterranean convective systems are also associated with intense hydrometeorological hazards, especially when short-duration rainfall cores interact with complex terrain [25].

The analysis relies on data from four rain gauges strategically distributed across the Metropolitan City of Naples (Table 1), providing coverage of the western sector (Pozzuoli), the central longitudinal sectors of Naples (plain and hill areas), and the eastern sector (Acerra).

The spatial configuration of the network (Figure 2) supports a local analysis of sub-hourly temporal structure while acknowledging that point gauges cannot fully resolve the spatial variability of convective cells [10,26]. All gauges operate at a 10 min recording

interval, which defines the minimum temporal resolution at which rainfall sub-events can be analyzed.

Table 1. Rain gauge network used in the study, including elevation and geographic coordinates.

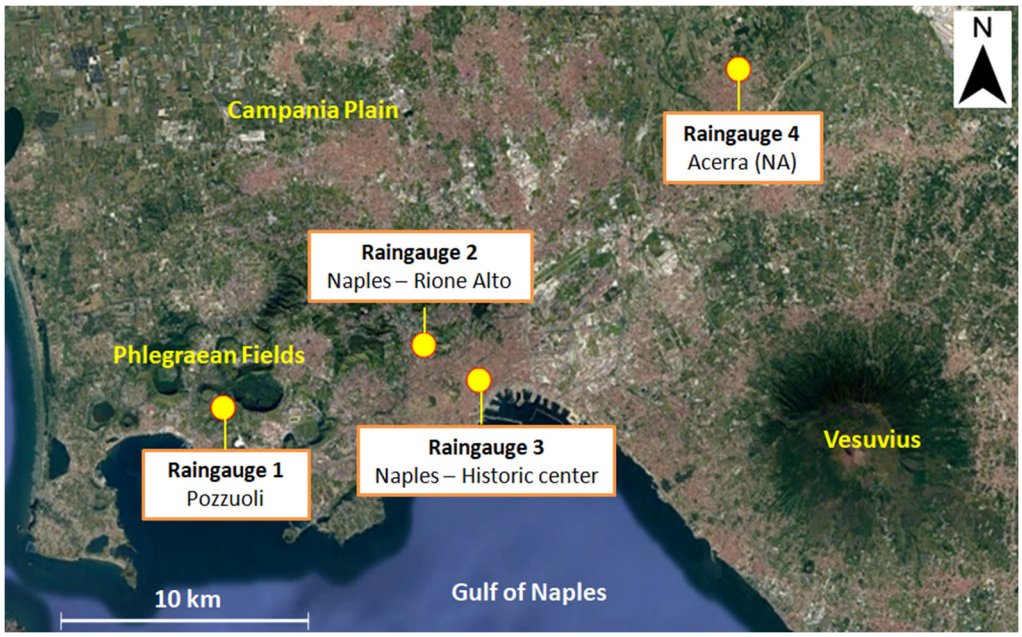

Rain Gauge	Elevation (m a.s.l.)	Latitude (° N)	Longitude (° E)
Pozzuoli (NA)	127	40°50′08″	14°07′51″
Rione Alto (Naples)	285	40°51′36″	14°13′34″
Historic center (Naples)	50	40°50′48″	14°14′57″
Acerra (NA)	30	40°57′05″	14°22′26″

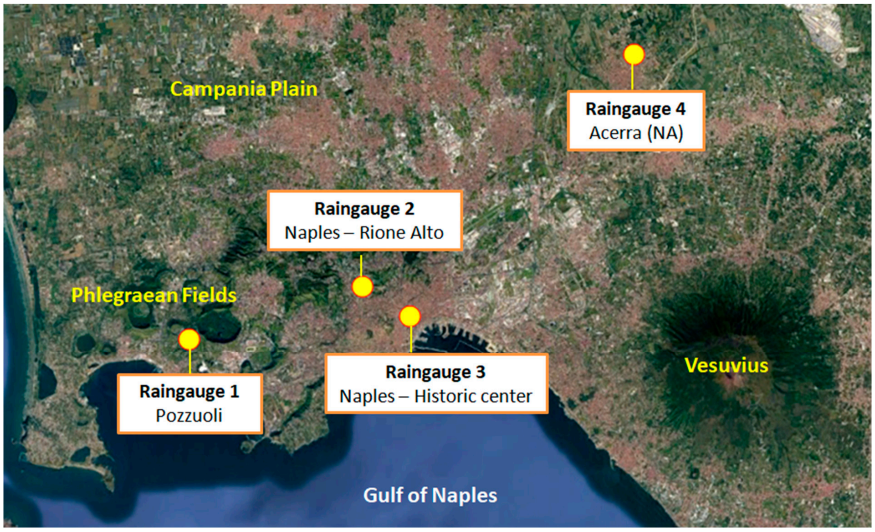

Figure 2. Spatial distribution of the four rain gauges used in the study across the Metropolitan City of Naples.

Short discontinuities due to missing data occur in some of the rainfall series. Although individual gaps were not systematically inspected, a limited number of rainfall events may

not have been captured. Any such loss is expected to be minor and to exert only a marginal influence on the event-based analyses carried out in this study.

All rainfall series underwent the standard quality-control workflow adopted by the Regional Functional Centers, including automated range and spike checks, temporal consistency verification, spatial coherence checks against neighboring stations, and removal of periods affected by sensor malfunction or maintenance. These procedures ensure that the extracted short-duration events are based on validated and physically consistent measurements. In line with the fast hydrological response typical of urban and peri-urban catchments, the analysis considers the 30, 40, 50 and 60 min durations, with particular emphasis on the shorter ones (30 and 40 min).

Although the number of rain gauges is admittedly limited, the decision to rely on only four instruments is intentional. Expanding the analysis to include additional gauges located around the study area would inevitably introduce orographic influences and other local conditioning factors whose contribution would be extremely difficult to quantify or isolate. In this sense, using four homogeneous gauges is preferable to incorporating five, six, or seven stations whose measurements would be conditioned by uncertain orography-driven variability.

Rainfall events were screened to identify 30 to 60 min sequences whose cumulative depths exceeded thresholds derived from regional DDF curves (VAPI procedure). The extraction procedure explicitly limits the multiple use of the same 10 min rainfall value across overlapping windows, preventing artificial inflation of event counts and ensuring that each selected event corresponds to a physically distinct convective core. The VAPI project, coordinated by the Consiglio Nazionale delle Ricerche—Gruppo Nazionale per la Difesa dalle Catastrofi Idrogeologiche (CNR-GNDCI), Perugia, Italy, provides a quasi-institutional framework for hydrometeorological hazard assessment in Italy and is widely used for the design and management of urban drainage systems and rainfall-induced hazards.

The VAPI–DDF curve is obtained from the corresponding IDF relationship by scaling the intensity through the event duration d. For the present study area (pluviometrically homogeneous sub-area A1), the base DDF curve—used without applying any K_T coefficient (K_T is the return-period growth factor)—is expressed as:

$$h(d) = \frac{77.08\, d}{\left(1 + \frac{d}{0.3661}\right)^{0.79089}} \quad (1)$$

where *h(d)* denotes rainfall depth (mm) for duration *d* (hours), and the parameters $\mu(I_0)$, dc, C, and D correspond to the calibrated values for the A1 sub-area (77.08, 0.3661, 0.7995, and 8.6077×10^{-5}, respectively). The variable z represents elevation above sea level and is set to an average value of 100 m for the present case study. The resulting base DDF curve is shown in Figure 3. This DDF relationship is used solely to define duration-consistent depth thresholds for event extraction and is not employed in the hydrological simulations.

The analysis begins at the 30 min duration because, with 10 min data resolution, only event durations of at least 30 min allow a meaningful assessment of the symmetry or asymmetry of the temporal distribution, a key descriptor of convective rainfall structure.

This study does not aim to determine sewer conduit sizing; instead, it evaluates the sensitivity of runoff generation to rainfall temporal distribution. The time of concentration (Tc) of the conceptual catchment used in the SWMM experiment is relatively short, equal to about 30 min. Tc was estimated using the Critical Storm Duration Method, which identifies the rainfall duration that maximizes peak discharge under controlled conditions. Although a rainfall duration equal to Tc would normally produce the largest peak discharge, peak

flow estimation lies outside the scope of this work. The focus is therefore placed on the internal temporal structure of short-duration rainfall events.

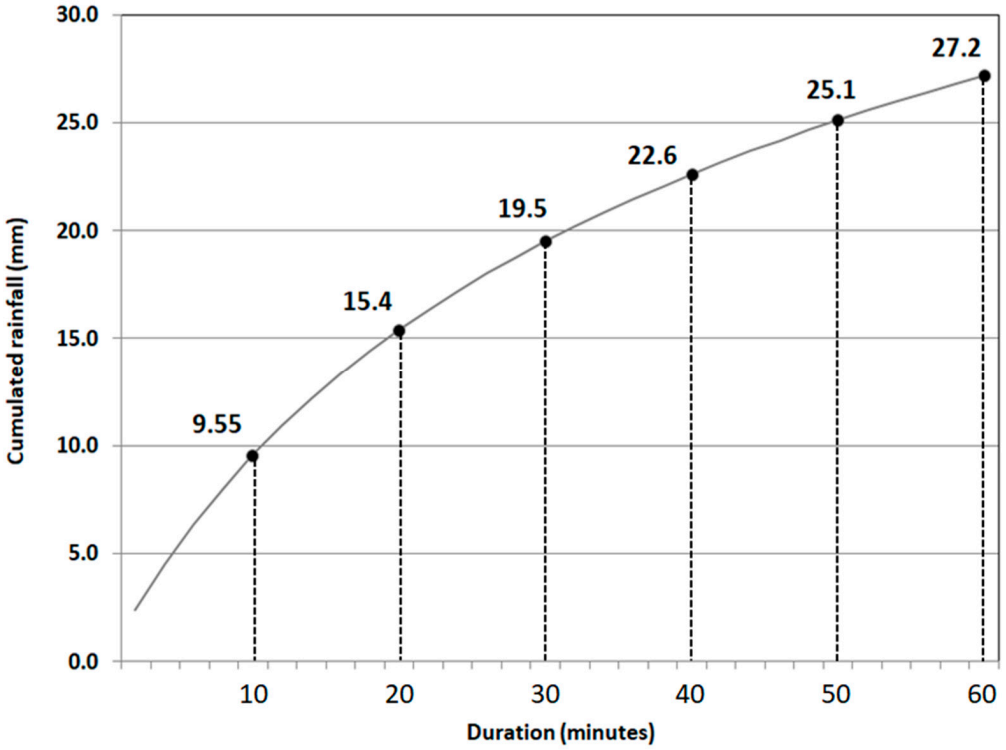

Figure 3. Base VAPI sub-hourly DDF curve (K_t = 1) derived from Equation (1) for sub-area A1.

2.2. Event Selection Procedure

The procedure adopted to identify significant short-duration rainfall events consists of four successive steps, each building on the previous one. Its purpose is to isolate well-defined events that are clearly separated from antecedent and subsequent precipitation and that exhibit internal homogeneity, without substantial pauses in rainfall intensity throughout their duration. To reduce partial-interval artifacts and better capture the temporal structure of each selected event, two additional 10 min intervals were appended to both the onset and decay phases during boundary refinement. This adjustment ensures that the extracted sequences fully represent the temporal variability of short-duration convective storms and provides a consistent basis for subsequent peak-intensity analyses. To avoid artificial inflation of event counts, the procedure limits the multiple use of the same 10 min rainfall value across overlapping windows, ensuring that each extracted sequence corresponds to a physically distinct convective core.

2.2.1. Preliminary Selection Based on DDF Thresholds

Sequences of consecutive 10 min intervals with total durations of 30, 40, 50, or 60 min were extracted (Figure 4). A sequence was retained if its cumulative rainfall exceeded the corresponding threshold derived from the official local DDF curves (VAPI method, with K_T = 1). This preliminary screening ensures that only events with rainfall volumes consistent with regional design-storm criteria are considered for further analysis. The 30 and 40 min events were subsequently used in the hydrological sensitivity experiment, whereas the 50 and 60 min durations were included solely in the rainfall analysis.

	A	B	C	D	E	F			
30-min	A_1	B_1	C_1				$A_1 + B_1 + C_1$	≥	**19.5**
40-min	A_2	B_2	C_2	D_2			$A_2 + B_2 + C_2 + D_2$	≥	**22.6**
50-min	A_3	B_3	C_3	D_3	E_3		$A_3 + B_3 + C_3 + D_3 + E_3$	≥	**25.1**
60-min	A_4	B_4	C_4	D_4	E_4	F_4	$A_4 + B_4 + C_4 + D_4 + E_4 + F_4$	≥	**27.2**

Figure 4. Extraction of 30, 40, 50, and 60 min sequences from consecutive 10 min intervals and comparison with the corresponding VAPI thresholds.

2.2.2. Definition of Onset and Decay Intervals

For each candidate event, the 10 min intervals immediately preceding and following the selected sequence were examined (Figure 5). The inner delimiting intervals were assigned a threshold equal to the difference between VAPI DDF depths for two consecutive durations, while the outer delimiting intervals were assigned half of this value. This criterion provides an objective and duration-consistent method for defining event boundaries.

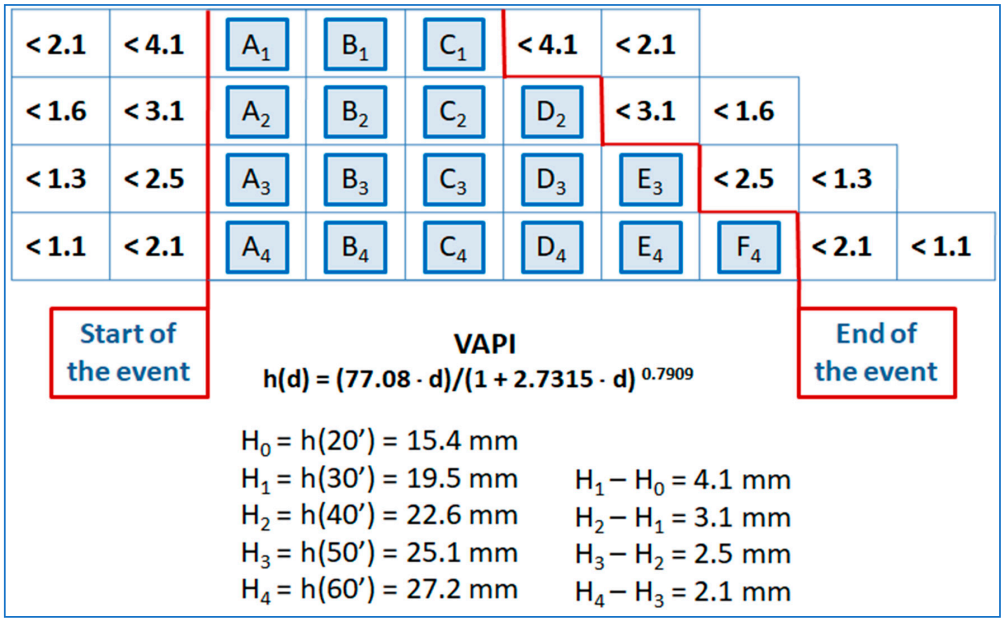

Figure 5. Thresholds used to define onset and decay intervals, derived from differences between consecutive VAPI depths and their halved values.

2.2.3. Internal Consistency Check

For each duration, the minimum 10 min accumulation within the event was identified (m_1–m_4), and the mean of the remaining intervals (Avg_1–Avg_4) was computed (Figure 6). Events were retained only if the ratio m/Avg exceeded a duration-specific threshold, ensuring that the selected sequences exhibited a coherent internal structure rather than isolated intensity spikes.

2.2.4. Boundary Interval Refinement

The two 10 min intervals adjacent to the event were required to have cumulative rainfall lower than the event's internal minimum (m_1–m_4). In addition, the outer delimiting intervals were required to be lower than half of this value (Figure 7). This condition

ensures a clear separation between the selected sub-hourly event and the surrounding low-intensity rainfall.

	A	B	C	D	E	F	
30-min	A_1	B_1	C_1				$\mathbf{m_1}$ = **Min** (A_1 ; B_1 ; C_1)
40-min	A_2	B_2	C_2	D_2			$\mathbf{m_2}$ = **Min** (A_2 ; B_2 ; C_2 ; D_2)
50-min	A_3	B_3	C_3	D_3	E_3		$\mathbf{m_3}$ = **Min** (A_3 ; B_3 ; C_3 ; D_3 ; E_3)
60-min	A_4	B_4	C_4	D_4	E_4	F_4	$\mathbf{m_4}$ = **Min** (A_4 ; B_4 ; C_4 ; D_4 ; E_4 ; F_4)

$\mathbf{Avg_1} = [(A_1 + B_1 + C_1 - \mathbf{m_1})]/2$	$\mathbf{m_1} / \mathbf{Avg_1} > 0.300$
$\mathbf{Avg_2} = [(A_2 + B_2 + C_2 + D_2 - \mathbf{m_2})]/3$	$\mathbf{m_2} / \mathbf{Avg_2} > 0.275$
$\mathbf{Avg_3} = [(A_3 + B_3 + C_3 + D_3 + E_3 - \mathbf{m_3})]/4$	$\mathbf{m_3} / \mathbf{Avg_3} > 0.250$
$\mathbf{Avg_4} = [(A_4 + B_4 + C_4 + D_4 + E_4 + F_4 - \mathbf{m_4})]/5$	$\mathbf{m_4} / \mathbf{Avg_4} > 0.225$

Figure 6. Minimum 10 min accumulation and internal mean computed for each event duration.

$< m_1/2$	$< \mathbf{m_1}$	A_1	B_1	C_1	$< \mathbf{m_1}$	$< m_1/2$		
$< m_2/2$	$< \mathbf{m_2}$	A_2	B_2	C_2	D_2	$< \mathbf{m_2}$	$< m_2/2$	
$< m_3/2$	$< \mathbf{m_3}$	A_3	B_3	C_3	D_3	E_3	$< \mathbf{m_3}$	$< m_3/2$
$< m_4/2$	$< \mathbf{m_4}$	A_4	B_4	C_4	D_4	E_4	F_4	$< \mathbf{m_4}$	$< m_4/2$
Start of the event							**End of the event**	

Figure 7. Boundary interval thresholds based on the event's internal minimum (m_1–m_4) and its halved value.

The screening procedure identified rainfall events with durations of 30, 40, 50, and 60 min. A total of 21 events were selected for the 30 min duration and 20 for the 40 min duration, while the number of events decreased markedly for the 50 and 60 min durations (eight and seven events, respectively). These selected events constitute the reference dataset for the present analysis. The complete event lists are omitted, as the analysis focuses on aggregated metrics—namely, the mean contribution of each 10 min sub-interval and the intensity ratios KMAv and KMm.

For each event, the rainfall depth of each 10 min sub-interval was normalized by the total event depth, yielding an event-specific percentage profile. KMAv is defined as the ratio between the maximum and mean 10 min percentage contribution, whereas KMm is the ratio between the maximum and minimum contribution. A comparison with a normalization applied to the ensemble-mean profile showed differences below 1.4%, confirming that the event-wise procedure does not affect the interpretation of KMAv and KMm. The resulting mean depth values and percentage contributions for each duration are reported in Table 2.

Table 2. Mean 10 min rainfall distribution for the selected real events. Values are reported as absolute depth (mm) and relative contribution (%). KMAv = maximum-to-mean ratio; KMm = maximum-to-minimum ratio.

Duration	1st 10-min	2nd 10-min	3rd 10-min	4th 10-min	5th 10-min	6th 10-min	Total (mm)	KMAv	KMm
30-min	8.80 (33.3%)	11.14 (41.9%)	6.66 (24.8%)	-	-	-	26.60	1.257	1.689
40-min	7.59 (26.5%)	9.73 (31.7%)	7.46 (24.2%)	5.45 (17.6%)	-	-	30.23	1.268	1.801
50-min	4.69 (13.8%)	7.04 (21.5%)	8.43 (24.5%)	9.24 (26.1%)	4.99 (14.1%)	-	34.39	1.305	1.891
60-min	4.42 (13.3%)	7.07 (21.0%)	5.41 (16.2%)	6.11 (18.3%)	5.70 (16.8%)	5.12 (14.4%)	33.83	1.260	1.579

The distribution of rainfall among the 10 min sub-intervals confirms that real events are highly irregular and far from constant in intensity. The KMAv ratio, expressing the relationship between the maximum and mean sub-interval percentage contributions, remains remarkably stable across durations, ranging between 1.25 and 1.35. In contrast, the KMm ratio, comparing the maximum and minimum sub-interval percentage contributions, varies between 1.50 and 1.90, highlighting the pronounced internal variability that characterizes short-duration convective storms. The stability of KMAv across durations and the broader variability of KMm indicate that convective storms consistently exhibit strong temporal concentration, with limited sensitivity to duration-specific sampling effects.

Based on the percentage contributions reported in Table 2, Table 3 presents the corresponding VAPI-generated rainfall amounts for each event duration, using growth factors K_T = 1.00 (base curve) and K_T = 1.22 (associated with a 5-year return period—RT).

Table 3. VAPI-generated rainfall depth for each event duration (K_T = 1.00 and K_T = 1.22), redistributed across 10 min sub-intervals according to the percentage structure of real events as reported in Table 2.

Duration	VAPI K_T = 1.00	VAPI K_T = 1.22	1st 10-min (mm)	2nd 10-min (mm)	3rd 10-min (mm)	4th 10-min (mm)	5th 10-min (mm)	6th 10-min (mm)	Total (mm)
30-min	19.5	23.8	7.93	9.97	5.90	-	-	-	**23.8**
40-min	22.6	27.6	7.31	8.75	6.68	4.86	-	-	**27.6**
50-min	25.1	30.6	4.22	6.58	7.50	7.99	4.31	-	**30.6**
60-min	27.2	33.2	4.42	6.97	5.38	6.08	5.58	4.77	**33.2**

3. Results

In the hydrological sensitivity experiment, only the 30 and 40 min events were used, whereas the 50 min duration was included solely to illustrate the progressive weakening of convective peak dominance. The 60 min duration is excluded because it does not meaningfully isolate the convective core. For each duration, events were normalized to allow comparison across different cumulative depths. The analysis reveals a clear and physically coherent transition from strongly concentrated convective profiles at shorter durations to more distributed structures at longer ones.

The rainfall partitioning over the 10 min sub-intervals highlights the marked intra-event variability typical of real storms, which seldom exhibit a uniform intensity profile. Yet, despite this variability, the KMAv ratio remains remarkably stable across durations, as analytically reported above. This stability indicates that short-duration convective storms share a characteristic internal organization, regardless of their total depth or length. In

contrast, the broader spread of KMm reflects the sharp intensity gradients that define these events and confirms that convective storms consistently exhibit strong temporal concentration, with limited sensitivity to duration-specific sampling effects. Similar behavior has been observed in hourly extremes, where peak intensities often exceed thermodynamic expectations and concentrate within narrow temporal windows [7].

In contrast, the KMm ratio spans a broader interval (1.50 to 1.90), underscoring the sharp intensity gradients that define these events. This behavior highlights the intrinsic complexity of sub-hourly convective rainfall, where brief but intense peaks dominate the internal dynamics. High-resolution convection-permitting simulations consistently reproduce these short-lived intensity bursts, confirming their role in shaping sub-hourly rainfall structure [8]. These ratios quantify the departure from uniform intensity and provide a direct link between observed rainfall structure and design-storm uncertainty [13,15,17]. These duration-dependent patterns provide a coherent framework for interpreting the internal organization of short-duration convective storms and set the stage for assessing how such structures relate to synthetic design profiles.

Overall, the results show that even within the natural variability of convective storms, their internal temporal structure exhibits recognizable and repeatable features. This reproducibility is consistent with the behavior of organized convective systems, which tend to exhibit stable internal timing even under varying environmental conditions [9]. This coherence strengthens the connection between real sub-hourly events and the synthetic profiles used in DDF-based design storms, offering a more informed basis for interpreting short-duration rainfall extremes.

3.1. Variability and Uncertainty of Mean Rainfall Profiles

To quantify the variability associated with the mean temporal structure of short-duration convective storms, uncertainty measures were computed for each 10 min interval across all selected 30 and 40 min events. Figures 8 and 9 report the mean rainfall depth together with ±1 standard deviation and the 95% confidence interval of the mean. The 30 min events display a distinctly central peak, whereas the 40 min storms exhibit an early-central maximum around the 20 min mark, with larger dispersion during the rising limb and reduced variability toward the decay phase. These aggregated results provide a statistical envelope for the temporal organization of 30 and 40 min convective storms and complement the event-based analyses presented in Sections 3.2 and 3.3.

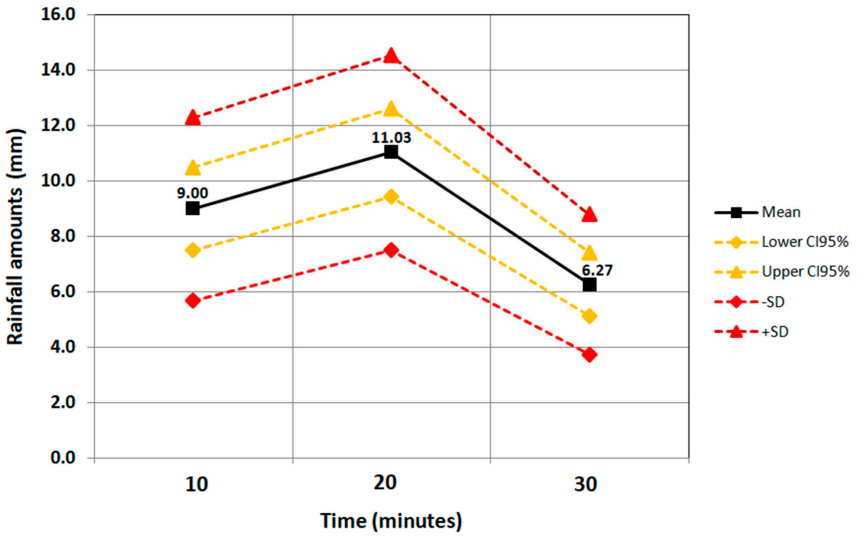

Figure 8. Mean rainfall profile for the 30 min events, including ±1 standard deviation and the 95% confidence interval of the mean.

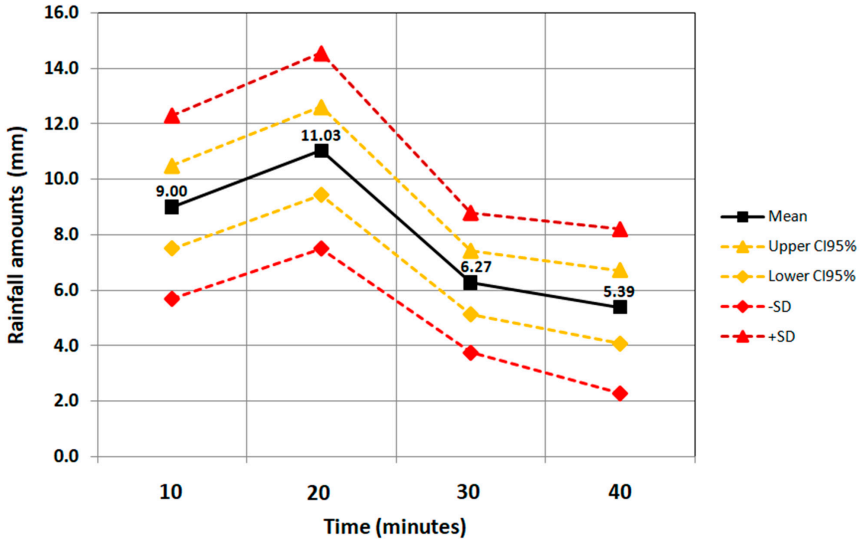

Figure 9. Mean rainfall profile for the 40 min events, including ±1 standard deviation and the 95% confidence interval of the mean.

3.2. Temporal Structure of 30-Min Events

A total of 21 events satisfied the selection criteria for the 30 min duration. Their internal structure exhibits a pronounced and highly consistent central peak: on average, the second 10 min interval contributes 41.9% of the total event depth, while the first and third intervals contribute 33.3% and 24.8%, respectively (Table 2). This pattern is remarkably stable across events and highlights the strongly convective nature of short-duration storms, in which the bulk of rainfall is concentrated within a narrow temporal window. High-resolution analyses indicate that these central peaks correspond to well-defined convective cores embedded within broader storm structures [22].

The polynomial fits shown in Figure 10 further emphasize this behavior. Both the third- and fourth-degree curves capture the steep ascent and asymmetric decay that characterize convective bursts, with rainfall intensity rising sharply toward the central portion of the event and then decaying more gradually. The resulting 30 min profile is sharply peaked and asymmetric, with a rapid rise followed by a more gradual decay.

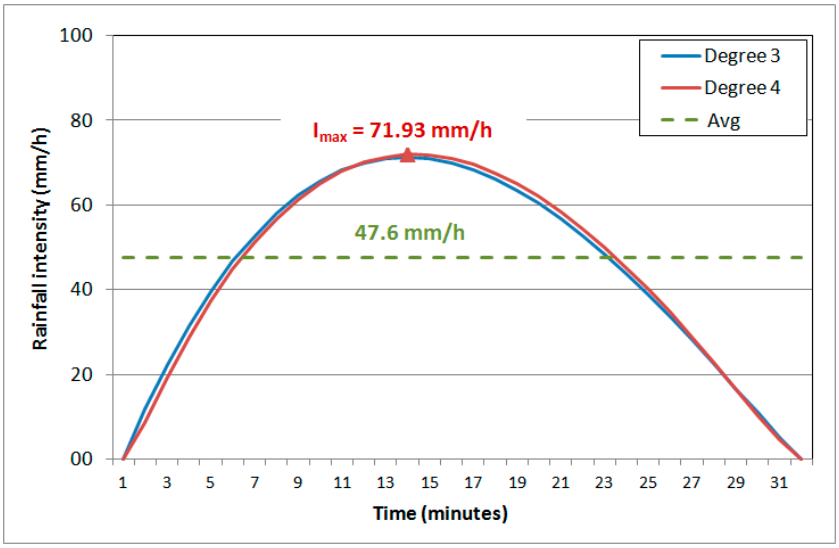

Figure 10. Third- and fourth-degree least-squares polynomial fits of a representative 30 min rainfall-intensity series. Both curves provide smoothed representations of the event and consistently capture the central intensity peak.

This structure aligns with the canonical behavior of short-duration convective storms, where the most intense precipitation is concentrated within a narrow temporal window [10,24,25]. The pronounced central peak and the steep intensity gradients observed here reinforce the distinctive internal organization of sub-hourly convective events.

Overall, the 30 min events display a distinctive internal signature, dominated by a short-lived but intense peak that governs the event's dynamics. This concentrated structure is a defining feature of sub-hourly convective rainfall and provides a physically meaningful reference for interpreting the variability observed at longer durations.

3.3. Temporal Structure of 40-Min Events

A total of 20 events met the selection criteria for the 40 min duration. Compared to the 30 min storms, their internal structure remains convective in nature but exhibits a more distributed pattern. On average, the second 10 min interval contributes 31.7% of the total event depth, followed by the first (26.5%), third (24.2%), and fourth (17.6%) intervals (Table 2).

This distribution indicates that the peak remains located in the early-central portion of the event, although it is less dominant than in the 30 min case. The non-negligible contribution of the fourth interval reflects a broader temporal spreading of rainfall intensity, consistent with longer-lived convective cells or the partial inclusion of dissipative phases. Such temporal spreading is consistent with longer-lived convective cells and with the partial inclusion of dissipative phases [11].

The polynomial fits shown in Figure 11 further emphasize this behavior. Both the fourth- and fifth-degree curves capture the more gradual intensity modulation that characterizes 40 min storms, with a smoother rise toward the central portion of the event and a slower decay thereafter. The close agreement between the two fits highlights the consistency of this internal organization across different smoothing approaches.

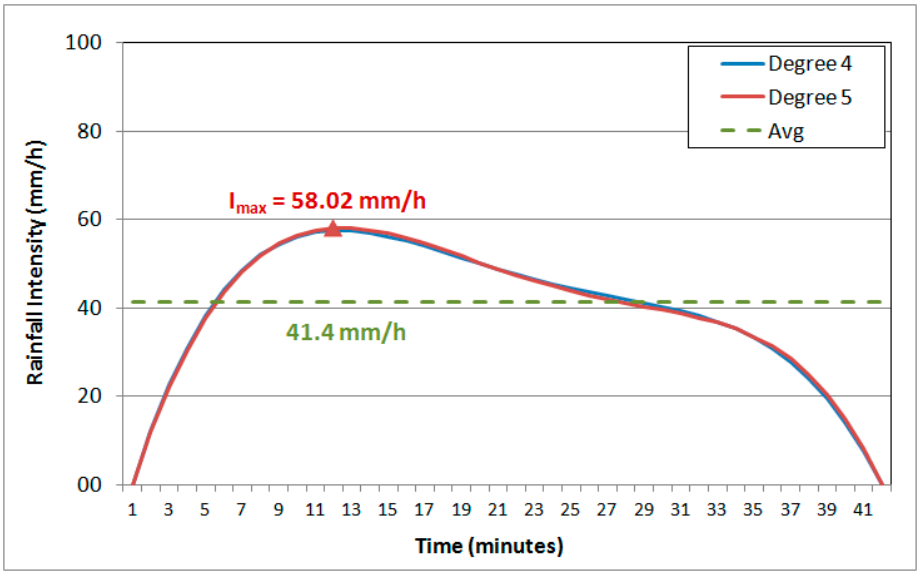

Figure 11. Fourth- and fifth-degree least-squares polynomial fits of a representative 40 min rainfall-intensity series. Both curves provide smoothed representations of the event and consistently capture the early-central intensity peak.

The intensity ratios support this interpretation. The KMAv value (1.268) indicates a moderate concentration around the peak, while the KMm ratio (1.801) confirms substantial variability between the most and least intense sub-intervals. Together, these metrics show

that 40 min events retain a convective signature, but with a more distributed temporal structure than their 30 min counterparts.

Overall, the 40 min events display a transitional internal organization: still convective, but with a wider temporal footprint. This shift marks the first step away from the sharply concentrated structure of shorter events and toward the smoother, more distributed profiles observed at longer durations.

3.4. Temporal Structure of 50-Min Events

The internal structure of the 50 min events shows a clear departure from the sharply concentrated profiles observed at shorter durations. The contributions across the five 10 min intervals are more balanced, and the absence of a dominant central peak indicates that these events are less representative of pure convective dynamics. This pattern reflects the increasing influence of stratiform or dissipative phases, which tend to reduce intensity contrasts and broaden the temporal footprint of the event. The intensity ratios further highlight this behavior. KMAv reaches its highest value (1.305), indicating a relatively modest contrast between the maximum and mean sub-interval depths, while KMm (1.891) reflects the presence of occasional intensity bursts embedded within otherwise smoother profiles. Together, these metrics confirm that 50 min events exhibit a transition toward mixed convective–stratiform structures, with a more uniform temporal distribution.

On this basis, the 50 min duration was excluded from further detailed analysis and from graphical representation, as its internal organization is no longer dominated by the convective core that characterizes sub-hourly extreme rainfall.

3.5. Comparative Analysis Across Durations

A clear and progressive transition emerges across the three analyzed durations (30, 40, and 50 min):

- 30 min events: strongly peaked and distinctly convective structure, with rainfall concentrated within a narrow temporal window,
- 40 min events: temporal concentration decreases, and events become less effective at isolating a single convective core. Temporal concentration decreases, and events become less effective at isolating a single convective core, as longer durations tend to dilute short, intense bursts embedded within real convective events,
- 50 min events: plateau-like distribution with a markedly weakened convective peak and broader temporal spreading.

This progression reflects the physical evolution of Mediterranean convective storms, whose core typically lasts 20 to 40 min. Durations exceeding this range increasingly incorporate stratiform or dissipative phases, which reduce intensity contrasts and weaken the dominance of the central peak. This behavior is consistent with the organization of convective systems, which often exhibit well-defined cores followed by dissipative tails [9].

These findings demonstrate that the bias introduced by constant-intensity design storms depends on the relationship between the selected duration and the physical duration of the convective core, particularly in small, highly responsive urban catchments sensitive to sub-hourly variability [11].

3.6. Implications for Peak-Runoff Estimation and Design-Storm Bias

The comparative analysis across durations reveals a physically consistent transition in storm behavior as event length increases from 30 to 50 min. This transition reflects the intrinsic dynamics of Mediterranean convective systems, whose cores typically last 20 to 40 min, and has direct implications for hydrological modeling and infrastructure design.

30- and 40 min events exhibit strongly peaked temporal structures, characterized by rapid intensification toward a central maximum followed by a more gradual decay. These profiles are dominated by short-lived convective bursts, with peak intensities substantially exceeding the event mean. Similar behavior has been documented in hourly extremes, where peak intensities frequently exceed thermodynamic expectations [7]. The high peak ratios and the central position of the temporal centroid confirm that these durations effectively isolate the convective core of Mediterranean storms. This behavior is consistent with previous studies documenting the temporal asymmetry and concentration typical of convective precipitation [5,10,24]. Convection-permitting simulations reproduce these sharply peaked structures, indicating that they are a recurrent feature of short-duration convective rainfall [8].

These findings highlight a fundamental limitation of constant-intensity design storms derived from DDF curves. While DDF depths are physically meaningful, the assumption of uniform intensity over the selected duration is not. Real convective storms concentrate rainfall within narrow temporal windows, and the bias introduced by constant-intensity storms increases when the selected duration exceeds the physical duration of the convective core. Longer uniform durations dilute short, intense bursts embedded within real events, leading to recurrent underestimation of peak intensities and, consequently, peak-runoff.

This has practical implications for infrastructure sizing and risk assessment. Such discrepancies may affect the ability of drainage systems, culverts, and retention basins to accommodate the true peak flows generated by convective storms, increasing the likelihood of flooding, surface runoff, and debris-flow initiation in susceptible areas. The issue is particularly relevant in small, highly responsive urban catchments, where peak discharge is strongly controlled by short-duration rainfall extremes.

Given the projected intensification of short-duration rainfall extremes under climate change [3,5,6], reliance on oversimplified design storms may further increase the vulnerability of Mediterranean urban and peri-urban areas. These results therefore underscore the need to incorporate realistic temporal patterns into design rainfall models and to select event durations that align with the physical timescale of convective processes rather than relying solely on DDF-based thresholds.

4. Hydrological Modeling with SWMM

4.1. Conceptual Catchment Configuration and Parameterisation

The SWMM modeling framework was designed to isolate the hydrological impact of rainfall temporal variability while avoiding unnecessary complexity in catchment representation. A conceptualized catchment was therefore adopted to ensure that differences in peak runoff could be attributed solely to the temporal organization of rainfall inputs rather than to uncertainties in model calibration or drainage-network heterogeneity. This approach is consistent with previous studies showing that short-duration convective storms exert a strong influence on peak-discharge generation in small urban basins. Urban hydrological response is particularly sensitive to sub-hourly rainfall variability, which makes simplified catchment configurations appropriate for isolating temporal effects [11].

The conceptual catchment represents a medium-sized peri-urban basin typical of Mediterranean metropolitan fringes, with a total drainage area of 6.0 ha. The area is subdivided into two aggregated land-use classes:

- impervious urban surfaces, characterized by rapid runoff production,
- pervious green or peri-urban areas, contributing delayed and attenuated flow.

Representative hydrological parameters were assigned following standard SWMM guidelines. The Horton infiltration model was adopted using conceptual parameter values representative of the hypothetical peri-urban catchment, ensuring consistent hydrological

conditions across all simulations. and flow routing was performed using the dynamic wave formulation. Impervious areas were characterized by a Manning's n of 0.013, while pervious areas were assigned a value of 0.15. Physiographic characteristics are summarized in Table 4, which provides the parameter set used for all simulations. Rainfall values from a single rain gauge have been adopted for the simulations.

Table 4. Physiographic characteristics of the conceptual peri-urban sub-catchments used in the SWMM simulations. Sub-catchment IDs adopt the suffix **i** for impervious units and **p** for pervious units.

Sub Catchment	Outlet	Area (ha)	Imperv. (%)	Width (m)	Slope (%)	Depression Storage	Zero Imp. Fraction
S01i	J01a	0.30	95	80	0.5	0.015	40
S10p	J01a	0.40	5	80	2.0	0.030	25
S11p	J01a	0.40	5	80	2.0	0.030	25
S02i	J02a	0.20	90	50	0.5	0.015	40
S03i	J02a	0.20	90	50	0.5	0.015	40
S05i	J10a	0.30	95	60	0.5	0.015	40
S04i	J09a	0.30	95	60	0.5	0.015	40
S06i	J13a	0.30	95	60	0.5	0.015	40
S07i	J14a	0.30	95	60	0.5	0.015	40
S08i	J13a	0.30	95	60	0.5	0.015	40
S09i	J14a	0.30	95	60	0.5	0.015	40
S12p	J08a	0.25	5	80	2.0	0.030	25
S16p	J08a	0.25	5	80	2.0	0.030	25
S20p	J12a	0.25	5	80	2.0	0.030	25
S13p	J03a	0.20	5	60	2.0	0.030	25
S17p	J05a	0.20	5	60	2.0	0.030	25
S14p	J07a	0.20	5	60	2.0	0.030	25
S18p	J05a	0.20	5	60	2.0	0.030	25
S22p	J07a	0.20	5	60	2.0	0.030	25
S15p	J11a	0.25	5	80	2.0	0.030	25
S19p	J11a	0.25	5	80	2.0	0.030	25
S23p	J15a	0.25	5	80	2.0	0.030	25

A highly schematic and symmetrical layout with multiple sub-catchments and conduits (Figure 12) has been adopted to facilitate a clear interpretation of the hydrological effects of rainfall temporal variability while avoiding unnecessary structural complexity. This simplified but physically meaningful configuration ensures that the hydrological response is driven primarily by rainfall-intensity patterns, providing a controlled environment for evaluating the influence of temporal variability.

Similar conceptual layouts have been used to evaluate the influence of rainfall temporal patterns on SWMM-based flood simulations [14]. By removing structural and calibration-related uncertainties, the modeling strategy highlights the extent to which constant-intensity design storms may underestimate peak flows compared with storms that preserve the observed temporal organization of rainfall. This underestimation is consistent with previous findings showing that uniform hyetographs tend to smooth out short convective bursts embedded within real events [13].

4.2. Rainfall Inputs and Simulation Setup

Two categories of rainfall inputs were used in the simulations: (a) constant-intensity design storms derived from DDF curves, and (b) variable-intensity storms preserving the observed temporal organization of real events.

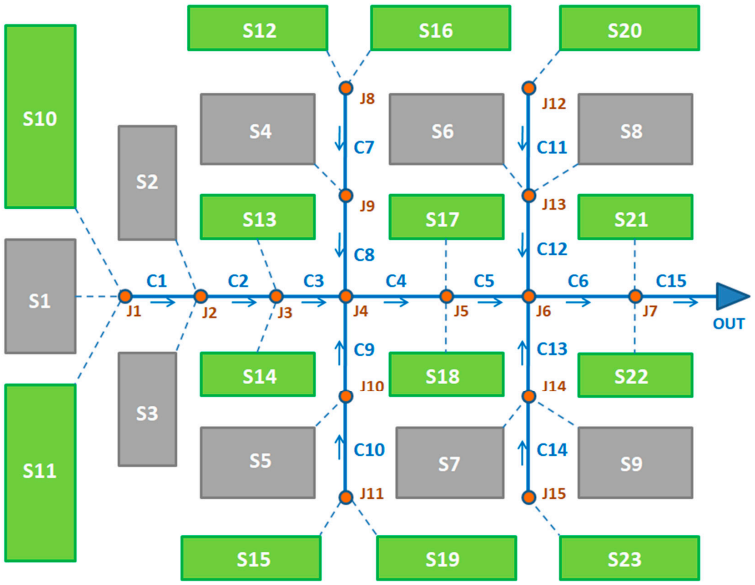

Figure 12. Schematic representation of the SWMM hydrological–hydraulic model. Sub-catchments (green: pervious; gray: impervious) discharge into junctions (J1–J15) through conduits (C1–C15), forming the simplified drainage network adopted for runoff routing. The outfall is completely free, without downstream backwater effects.

4.2.1. Constant-Intensity Design Storms

Constant-intensity storms were derived from the local Depth–Duration–Frequency (DDF) curves for event durations of 30 and 40 min. For each duration, the total rainfall depth associated with the selected return period (5 years, coefficient K_T = 1.22) was uniformly distributed over the storm duration, following standard design-storm practice. These storms provide a benchmark representation in which rainfall intensity is constant throughout the event. In addition to the DDF constant-intensity hyetographs, a persistence baseline was included, defined as a constant-intensity storm constructed using the mean rainfall intensity of the observed event.

4.2.2. Variable-Intensity Design Storms

Variable-intensity storms were constructed using the normalized temporal profiles obtained from the analysis of observed rainfall events. For each duration, the corresponding normalized profile was scaled to match the DDF-based design depth, ensuring that constant- and variable-intensity storms share the same cumulative rainfall and differ only in their internal temporal distribution. High-resolution modeling studies indicate that preserving the internal temporal organization of convective storms is important for reproducing realistic peak intensities [8]. This follows the logic of equal-volume hyetograph comparisons [13,15]. Three configurations were analyzed:

1. Variable-intensity storms based on normalized profiles extracted from observed events (Sections 3.2 and 3.3).
2. For 30 min storms, rainfall distributions obtained from cubic and quartic least-squares polynomial fits.
3. For 40 min storms, rainfall distributions obtained from quartic and fifth-degree least-squares polynomial fits.

These fitted profiles reflect the organized structure of Mediterranean convective systems [9]. The variable-intensity storms reproduce the steep ascent, central peak, and asymmetric decay typical of Mediterranean convective rainfall, providing a physically realistic counterpart to the uniform DDF-based storms.

4.3. Interpretation Framework

All simulations were performed using a 1 min computational time step, ensuring adequate resolution of short-duration convective peaks. Initial soil moisture and storage conditions were set to nominal values representative of moderate antecedent wetness, as the focus of the study is on relative differences between rainfall structures rather than on absolute flow magnitudes. This relative-difference approach aligns with previous analyses showing that peak discharge is strongly influenced by rainfall temporal variability [11]. For each duration (30- and 40 min), four simulations were run:

1. One constant-intensity storm
2. Three variable-intensity storms.

Peak discharge (Qp) and time to peak (Tp) were extracted at conduits C1 and C15, the latter conveying flow to the outlet node, to evaluate differences in peak-flow generation among the four storm configurations.

SWMM simulations were performed for all four rainfall laws: (i) A constant-intensity storm over the entire event duration; (ii) a storm with constant intensity within each of the 3–4 10 min sub-events; (iii) polynomial-fit storms using 3rd- and 4th-degree polynomials for the 30 min events; and (iv) 4th- and 5th-degree polynomial fits for the 40 min events. Since the polynomial fitting curves are almost always practically overlapping, for simplicity and graphical clarity only the curve exhibiting the higher peak value between the two was plotted.

5. Results—Hydrological Response Simulated with SWMM

This section compares the hydrological response of the conceptual catchment under constant- and variable-intensity design storms for durations of 30 and 40 min. For each duration, the total rainfall depth was kept identical between storm types, allowing the analysis to isolate the effect of temporal rainfall distribution on peak-flow generation.

5.1. General Behavior of the Hydrographs

Across both durations, hydrographs generated by variable-intensity storms exhibit:

(a) higher peak flow rates (Qp),
(b) shorter times to peak (Tp),
(c) steeper rising limbs,

when compared to those produced by constant-intensity storms.

This behavior reflects the strong temporal concentration typical of convective rainfall: intense bursts occurring within narrow time windows translate efficiently into rapid runoff generation in small, fast-response catchments. Urban hydrological response is particularly sensitive to sub-hourly rainfall variability [11]. In contrast, constant-intensity storms distribute rainfall uniformly over the event duration, producing smoother hydrographs with lower peaks and delayed responses. Similar findings have been reported in SWMM-based analyses showing that uniform hyetographs systematically underestimate peak flows [14]. This difference is consistent with the role of temporal rainfall concentration in controlling peak timing and magnitude. High-resolution modeling studies indicate that preserving convective peaks is important for reproducing realistic hydrograph dynamics [8].

5.2. 30-Min Storms

For the 30 min duration, the contrast between constant- and variable-intensity storms is the most pronounced. The variable-intensity storm, characterized by a sharp early-central peak, produces a substantially higher peak discharge (Qp) due to the strong synchronization between rainfall intensity and the catchment concentration time. The steep rising limb

of the hyetograph aligns closely with the characteristic response time of the conceptual basin, resulting in an efficient translation of rainfall into runoff (Figures 13 and 14). This synchronization effect is consistent with previous analyses showing that short-duration convective bursts dominate peak flow generation [13].

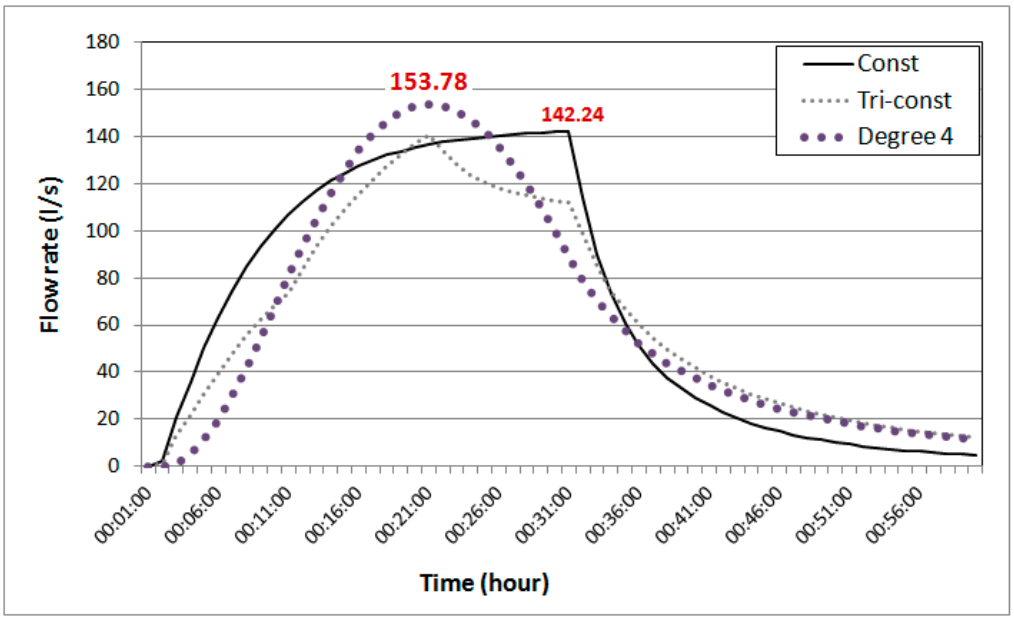

Figure 13. Hydrological response at conduit C01 under the 30 min design storms. The comparison between constant- and variable-intensity hyetographs highlights the strong influence of rainfall temporal concentration on local flow response, with variable-intensity inputs producing higher peaks and steeper rising limbs.

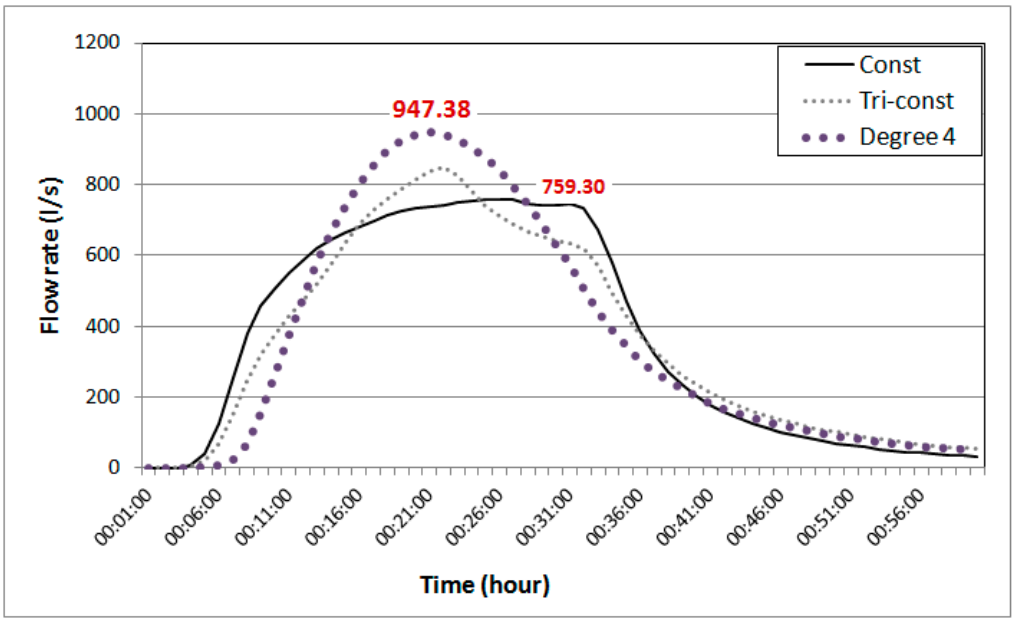

Figure 14. Hydrological response at conduit C15 under the 30 min design storms. Outlet hydrographs exhibit markedly higher peak flows and shorter times to peak under temporally concentrated rainfall inputs, confirming the dominant role of intensity bursts in driving peak discharge at the basin outlet.

This behavior aligns with the temporal organization observed in real Mediterranean convective events, where intense rainfall bursts occur within short intervals and rapidly generate runoff in small catchments [10,18]. Organized convective systems often exhibit sharply peaked cores lasting 20–40 min, reinforcing the relevance of this duration [9]. The

30 min simulations therefore highlight the strong sensitivity of peak-flow generation to rainfall temporal concentration, indicating that short-duration convective storms are poorly represented by uniform design hyetographs.

Constant-intensity storms systematically underestimate peak discharge because their uniform rainfall rate fails to reproduce the short, intense convective burst that governs real events. As a result, hydrographs exhibit lower peaks and delayed responses, demonstrating that short-duration convective storms cannot be adequately represented by uniform design hyetographs in fast-response catchments.

5.3. 40-Min Storms

For the 40 min duration, the variable-intensity storm still produces a higher peak discharge than the constant-intensity storm, although the relative difference is smaller than in the 30 min case. This behavior reflects the broader but still convective structure of 40 min events, where the central peak remains dominant but is less sharp and more temporally distributed.

The variable-intensity storm maintains a more efficient synchronization between rainfall intensity and catchment response time, generating a steeper rising limb and a shorter time to peak (Tp). However, the presence of a fourth 10 min interval with non-negligible contribution dilutes the temporal concentration relative to the 30 min storms, reducing—but not eliminating—the contrast with the constant-intensity scenario. This reduced contrast aligns with the broader temporal footprint typical of longer convective events (Figures 15 and 16).

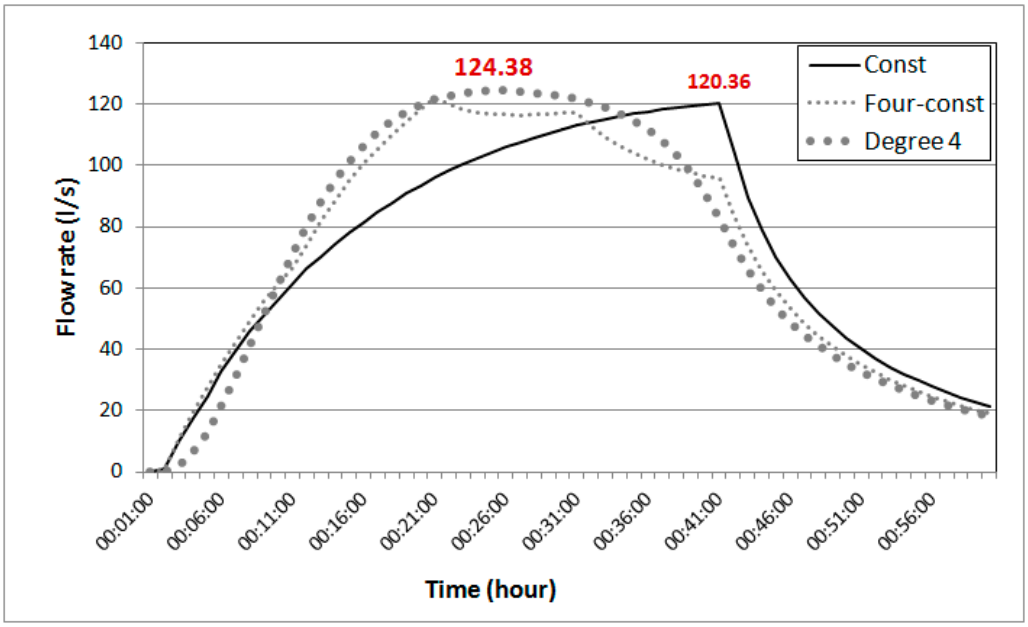

Figure 15. Hydrological response at conduit C01 for the 40 min design storms. The variable-intensity hyetographs yield higher peak discharges and steeper rising limbs than the constant-intensity storm, although the amplification is smaller than for 30 min storms.

Overall, the 40 min simulations indicate that convective dynamics remain influential at this duration, but the hydrological response becomes progressively less sensitive to peak intensification as the rainfall structure broadens. The reduced contrast between constant- and variable-intensity storms therefore reflects the transition toward more distributed rainfall profiles, consistent with the physical organization of longer convective events.

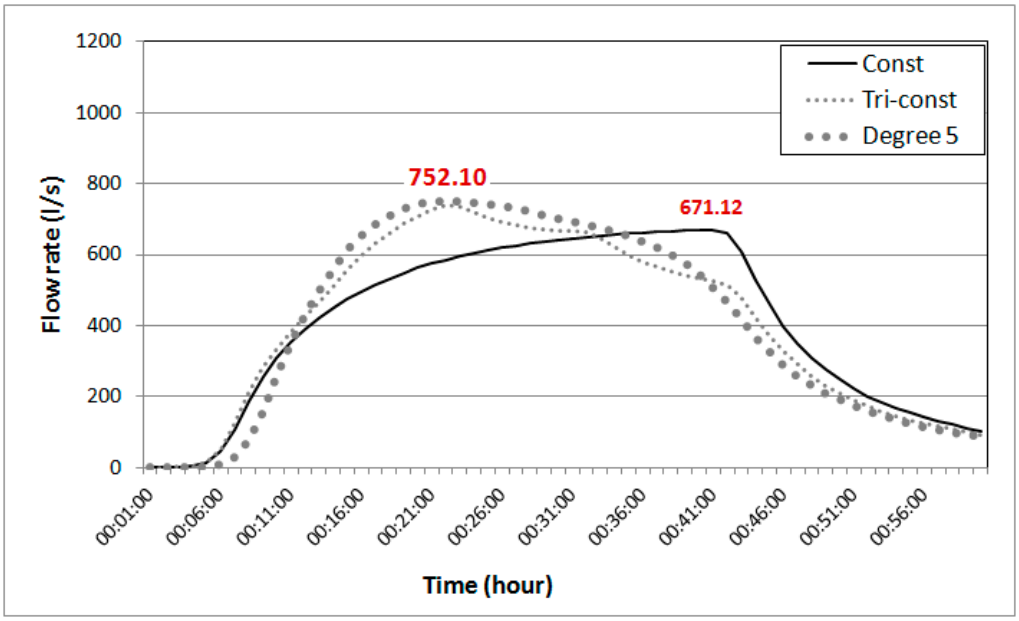

Figure 16. Hydrological response at conduit C15 for the 40 min design storms. Outlet response remains sensitive to hyetograph shape, with variable-intensity inputs producing earlier and higher peaks than the constant-intensity storm.

5.4. Detailed Comparison of Hydrographs and Peak-Discharge Ratios

The hydrograph generated by the variable-intensity storm exhibits a rapid rise, a well-defined peak, and a gradual recession, whereas the constant-intensity storm produces a flatter and more symmetrical response. SWMM simulations confirm that preserving temporal variability is important for reproducing realistic peak discharge behavior [14]. These differences confirm that 40 min storms still capture the convective core and that the internal temporal structure remains critical for peak-flow estimation.

Tables 5 and 6 summarize peak discharges, peak times, and peak-flow ratios for the 30 and 40 min design storms. The highest ratios occur for the 30 min events, reflecting the closer alignment between rainfall concentration and the response time of the conceptual catchment.

Table 5. Peak discharge (Q_p), time to peak (T_p), and peak-flow ratios for the 30 min design storms (Conduits C01–C15).

Rainfall-Intensity Distribution	C01 Q_p (L/s)	T_p (min)	C15 Q_p (L/s)	T_p (min)
Constant	142.24	31	759.30	31
Tri-constant	140.91	21	851.27	22
Degree-3 fit	152.09	21	936.43	21
Degree-4 fit	153.78	22	947.38	21
Max ratio	**1.09**	–	**1.25**	–

The results clearly show that:

- 30 min storms produce the largest relative differences between constant- and variable-intensity configurations, due to the strong synchronization between rainfall peaks and the catchment concentration time;
- 40 min storms still exhibit sensitivity to temporal structure, but the relative amplification of peak flows is smaller.

Table 6. Peak discharge (Q_p), time to peak (T_p), and peak-flow ratios for the 40 min design storms (Conduits C01–C15).

Rainfall-Intensity Distribution	C01 Q_p (L/s)	T_p (min)	C15 Q_p (L/s)	T_p (min)
Constant	120.36	41	671.12	41
Quadri-constant	121.95	21	740.89	22
Degree-4 fit	124.38	25	747.66	23
Degree-5 fit	124.17	24	752.10	22
Max ratio	**1.03**	–	**1.12**	–

The peak-flow ratio decreases with increasing duration, confirming that the hydrological impact of temporal concentration is strongest when the storm duration closely matches the catchment response time.

Overall, these results indicate that the internal temporal structure of convective storms plays a decisive role in peak-runoff generation, and that constant-intensity design storms fail to capture this behavior.

As discussed in Section 3.4, the 50 min duration was excluded from SWMM simulations because its internal temporal structure is no longer dominated by a convective core, making it unsuitable for evaluating peak-flow sensitivity to temporal concentration.

6. Discussion

High-resolution modeling further indicates that preserving temporal concentration is essential for reproducing realistic peak flows [7], consistent with recent findings showing that hourly extremes intensify at rates exceeding thermodynamic expectations [3,4,27]. This leads to systematic underestimation of peak runoff, especially in small and highly impervious urban catchments where sub-hourly rainfall dynamics dominate the hydrological response. These concerns are amplified under climate-change scenarios, which project more frequent and intense short-duration convective events [5,6,26]. The findings of this study highlight important implications for hydrological design, flood-risk assessment, and the sizing of urban drainage systems.

Real convective storms exhibit strong temporal concentration—particularly for durations of 30–40 min—that is not captured by constant-intensity design storms derived from DDF curves. This limitation aligns with previous evidence showing that short-duration extremes are governed by highly concentrated convective pulses, a tendency expected to intensify under future climatic conditions [13–15]. For 50 min events, differences tend to diminish because rainfall profiles become more distributed and may include stratiform, dissipative, or multicell components; given the limited number of observed 50 min storms, this duration should be considered indicative rather than conclusive.

Urban drainage networks—particularly those serving compact residential or commercial areas—are highly sensitive to short, intense convective pulses, and even modest variations in temporal rainfall structure can produce substantial increases in peak flow. This suggests that current design practices may underestimate the frequency and magnitude of surcharge events, surface flooding, and combined-sewer overflow [22]. High-resolution event identification also indicates that convective cores often occur as short-lived bursts embedded within multi-phase storms [5]. The comparison between constant- and variable-intensity storms demonstrates that peak-flow underestimation is most pronounced for durations aligned with the typical timescale of convective cores (30–40 min), consistent with recent analyses showing that sub-hourly extremes are strongly influenced by storm microphysics and convective organization [5,20]. These profiles should complement DDF/IDF depths rather than replace frequency analysis, improving design procedures

by more faithfully representing the internal dynamics of convective storms. Duration selection must also reflect storm physics: durations exceeding 40–50 min increasingly incorporates non-convective components, diluting the peak intensities that drive critical hydrological responses.

Selecting design durations solely based on DDF curves may therefore lead to storms that do not correspond to the physical timescale of the most impactful rainfall processes. A more physically informed approach—aligned with the typical duration of convective cores—can significantly enhance the representativeness of design storms and enhance the reliability of hydrological design under present and future climatic conditions [14]. The results support the adoption of temporally realistic synthetic hyetographs—such as Chicago hyetographs, Huff curves, beta-distribution-based profiles, or, preferably, site-specific profiles derived from high-resolution rainfall data.

7. Conclusions

This study demonstrates that the internal temporal structure of short-duration convective storms exerts a decisive influence on peak-runoff generation. The analysis of 30 min and 40 min events shows that Mediterranean convective storms are characterized by marked temporal concentration, with a substantial fraction of total rainfall occurring within a narrow central window. These durations align with the typical lifecycle of convective cores and therefore produce the strongest hydrological response.

As storm duration increases to 50 min, rainfall profiles become more distributed and may include stratiform, dissipative, or multicell components. This transition reduces the concentration of runoff generation and attenuates peak flows, underscoring the importance of selecting analysis durations that are physically consistent with convective dynamics rather than relying solely on thresholds derived from DDF curves. Physically meaningful durations ensure that design storms capture the temporal concentration that governs hydrological response in small, fast-responding catchments.

Hydrological simulations indicate that, in the large majority of cases, constant-intensity design storms underestimate peak discharge compared to variable-intensity storms with identical total depth. The largest discrepancies occur for 30 min and 40 min events, where sharp rainfall concentration drives rapid runoff accumulation and short times to peak. These results show that rainfall temporal structure is a primary control on peak-runoff estimation.

Although the analysis focuses on 30, 40, and 50 min storms, these durations should not be interpreted as strict boundaries. Convective systems may occasionally produce longer events—such as Mesoscale Convective Systems (MCS) or Mesoscale Convective Complexes (MCC)—with lifecycles lasting several hours and exhibiting temporal concentration comparable to that of short-duration storms. Multi-pulse or two-pulse storms may also generate multiple rainfall peaks within the same event. From a meteorological perspective, the study of convective-storm temporal structure is becoming increasingly important, as enhanced boundary-layer energy favors the development of more organized and longer-lived convective systems. These structures represent a major source of hydrometeorological hazard, and understanding their temporal organization is essential for improving the meteo-climatic resilience of urban environments.

Overall, the study provides quantitative evidence that incorporating realistic temporal patterns—whether derived from high-resolution observations or represented through synthetic hyetographs that mimic convective behavior—can substantially improve the reliability of hydrological design. This is particularly relevant for small and highly impervious urban catchments, where short-duration convective bursts dominate system response and where undersized infrastructure may lead to frequent surcharge, surface flooding, and

service disruption. As climate change is expected to intensify short-duration extremes, integrating temporal rainfall structure into design-storm construction represents an essential component of resilient urban-drainage planning.

Limitations and Future Work

The analysis is based on four rain gauges and on the events automatically isolated by the four-step selection procedure. The dataset is largely represented by 41 storms of 30 and 40 min duration, whereas only 15 storms of 50 and 60 min duration satisfy all selection criteria, which reduces the statistical robustness of the longer-duration profiles. The SWMM model used in this study is conceptual and intentionally uncalibrated; therefore, absolute discharge values should not be interpreted as predictions for any specific drainage network but rather as controlled comparisons of hydrological sensitivity to temporal rainfall structure.

Future work should expand the observational dataset, incorporate bootstrap confidence intervals for dimensionless hyetographs, and compare the event-selection procedure with MIET-based extraction to assess methodological consistency. Additional efforts should include testing radar-derived rainfall fields to capture spatial variability, evaluating multiple real drainage systems with differing imperviousness, slopes, storage capacities, and concentration times, and exploring the performance of alternative synthetic hyetographs under climate-change scenarios. Such developments would strengthen the generality of the findings and support the integration of temporally realistic design storms into engineering practice.

Author Contributions: Conceptualization, A.F.; methodology, A.F.; software, A.F.; validation, A.F.; formal analysis, A.F.; resources, A.F.; data curation, A.F.; writing—original draft preparation, A.F.; writing—review and editing, A.F. and F.M.; visualization, A.F.; supervision, F.M. All authors have read and agreed to the published version of the manuscript.

Funding: This research received no external funding. The research has been funded by the CNR-ISMAR own resources.

Data Availability Statement: The raw data supporting the conclusions of this article will be made available by the authors on request.

Acknowledgments: The management of the coastal weather station are within the frame of the CNR-ISMAR Marine Observing System (SOM). During the preparation of this manuscript, the authors used Microsoft 365 Copilot GPT 5.6 for the purposes of refining the text. The authors have reviewed and edited the output and take full responsibility for the content of this publication.

Conflicts of Interest: The authors declare no conflicts of interest. The funders had no role in the design of the study; in the collection, analyses, or interpretation of data; in the writing of the manuscript; or in the decision to publish the results.

References

1. Cavalleri, F.; Lussana, C.; Viterbo, F.; Brunetti, M.; Bonanno, R.; Manara, V.; Lacavalla, M.; Maugeri, M. Hourly Precipitation Patterns and Extremization over Italy Using Convection-Permitting Reanalysis Data. *Nat. Hazards Earth Syst. Sci.* **2026**, *26*, 279–297. [CrossRef]
2. Llasat, M.C.; del Moral, A.; Cortès, M.; Rigo , T. Convective precipitation trends in the Spanish Mediterranean region. *Atmos. Res.* **2021**, *257*. [CrossRef]
3. Westra, S.; Fowler, H.J.; Evans, J.P.; Alexander, L.V.; Berg, P.; Johnson, F.; Kendon, E.; Lenderink, G.; Roberts, N. Future Changes to the Intensity and Frequency of Short-Duration Rainfall Extremes. *Rev. Geophys.* **2014**, *52*, 522–555. [CrossRef]
4. Donat, M.G.; Lowry, A.L.; Alexander, L.V.; O'Gorman, P.A.; Maher, N. More Extreme Precipitation in the World's Dry and Wet Regions. *Nat. Clim. Change* **2016**, *6*, 508–513. [CrossRef]
5. Fowler, H.J.; Lenderink, G.; Prein, A.F.; Westra, S.; Allan, R.P.; Ban, N.; Barbero, R.; Berg, P.; Blenkinsop, S.; Do, H.X.; et al. Anthropogenic Intensification of Short-Duration Rainfall Extremes. *Nat. Rev. Earth Environ.* **2021**, *2*, 107–122. [CrossRef]

6. Marra, F.; Koukoula, M.; Canale, A.; Peleg, N. Predicting Extreme Sub-Hourly Precipitation Intensification Based on Temperature Shifts. *Hydrol. Earth Syst. Sci.* **2024**, *28*, 375–389. [CrossRef]
7. Lenderink, G.; van Meijgaard, E. Increase in Hourly Precipitation Extremes Beyond Expectations from Temperature Scaling. *Nat. Geosci.* **2008**, *1*, 511–514. [CrossRef]
8. Prein, A.F.; Langhans, W.; Fosser , G.; Ferrone , A.; Ban, N.; Goergen, K.; Keller, M.; Tölle, M.; Gutjahr, O.; Feser, F.; et al. A Review on Regional Convection-Permitting Climate Modeling: Demonstrations, Prospects, and Challenges. *Rev. Geophys.* **2015**, *53*, 323–361. [CrossRef]
9. Prein, A.F.; Rasmussen, R.M.; Ikeda, K.; Liu , C.; Clark, M.P.; Holland, G.J. The Future Intensification of Hourly Precipitation Extremes. *Nat. Clim. Change* **2017**, *7*, 48–52. [CrossRef]
10. Berne, A.; Delrieu, G.; Creutin, J.-D.; Obled, C. Temporal and Spatial Resolution of Rainfall Measurements Required for Urban Hydrology. *J. Hydrol.* **2004**, *299*, 166–179. [CrossRef]
11. Cristiano, E.; ten Veldhuis, M.-C.; van de Giesen, N. Spatial and Temporal Variability of Rainfall and Their Effects on Hydrological Response in Urban Areas—A Review. *Hydrol. Earth Syst. Sci.* **2017**, *21*, 3859–3871. [CrossRef]
12. Krvavica, N.; Rubinić, J. Evaluation of Design Storms and Critical Rainfall Durations for Flood Prediction in Partially Urbanized Catchments. *Water* **2020**, *12*, 2044. [CrossRef]
13. Pritsis, S.; Pons, V.; Rokstad, M.M.; Clemens-Meyer, F.H.L.R.; Kleidorfer, M.; Tscheikner-Gratl, F. The Role of Hyetograph Shape and Designer Subjectivity in the Design of an Urban Drainage System. *Water Sci. Technol.* **2024**, *90*, 920–934. [CrossRef]
14. Chen, J.; Li, Y.; Zhang, S. Impact of Different Design Rainfall Pattern Peak Factors on Urban Flooding. *Water* **2023**, *15*, 2468. [CrossRef]
15. Zhou, Z.; Smith, J.A.; Baeck, M.L.; Wright, D.B.; Smith, B.K.; Liu, S. The Impact of the Spatiotemporal Structure of Rainfall on Flood Frequency over a Small Urban watershed: An Approach Coupling Stochastic Storm Transposition and Hydrologic Modeling. *Hydrol. Earth Syst. Sci.* **2021**, *25*, 4701–4717. [CrossRef]
16. Keifer, C.J.; Chu, H.H. Synthetic Storm Pattern for Drainage Design. *J. Hydraul. Div. (ASCE)* **1957**, *83*, 1–25. [CrossRef]
17. Huff, F.A. Time Distribution of Rainfall in Heavy Storms. *Water Resour. Res.* **1967**, *3*, 1007–1019. [CrossRef]
18. Balbastre-Soldevila, R.; García-Bartual, R.; Andrés-Doménech, I. A Comparison of Design Storms for Urban Drainage System Applications. *Water* **2019**, *11*, 757. [CrossRef]
19. Peleg, N.; Marra , F.; Fatichi, S.; Molnar, P.; Morin, E.; Sharma, A.; Burlando, P. Intensification of Convective Rain Cells at Warmer Temperatures Observed from High-Resolution Weather Radar Data. *J. Hydrometeorol.* **2018**, *19*, 715–726. [CrossRef]
20. Brasil, J.; Guerreiro, M.S.; Andrade, E.M.; de Queiroz Palácio, H.A.; Medeiros, P.H.A.; Ribeiro Filho, J.C. Minimum Rainfall Inter-Event Time to Separate Rainfall Events in a Low Latitude Semi-Arid Environment. *Sustainibility* **2022**, *14*, 1721. [CrossRef]
21. Dunkerley, D. Rain Event Properties in Nature and in Rainfall Simulation Experiments: A Comparative Review with Recommendations for Increasingly Systematic Study and Reporting. *Hydrol. Process.* **2008**, *22*, 4415–4435. [CrossRef]
22. Peleg, N.; Morin , E. Convective rain cells: Radar-derived spatiotemporal characteristics and synoptic patterns over the eastern Mediterranean. *J. Geophys. Res. Atmos.* **2012**, *117*, D15116. [CrossRef]
23. Belda, M.; Holtanová, E.; Halenka, T.; Kalvová, J. Climate Classification Revisited: From Köppen to Trewartha. *Clim. Res.* **2014**, *59*, 1–13. [CrossRef]
24. Marra, F.; Armon, M.; Morin, E. Coastal and orographic effects on extreme precipitation revealed by weather radar observations. *Hydrol. Earth Syst. Sci.* **2022**, *26*, 1439–1458. [CrossRef]
25. Belachsen, I.; Marra, F.; Peleg, N.; Morin, E. Convective Rainfall in a Dry Climate: Relations with Synoptic Systems and Flash-Flood Generation in the Dead Sea Region. *Hydrol. Earth Syst. Sci.* **2017**, *21*, 5165–5180. [CrossRef]
26. Maier , R.; Krebs, G.; Pichler, M.; Muschalla, D.; Gruber, G. Spatial Rainfall Variability in Urban Environments: High-Density Precipitation Measurements on a City-Scale. *Water* **2020**, *12*, 1157. [CrossRef]
27. Pendergrass, A. What Precipitation Is Extreme? *Science* **2018**, *360*, 1072–1073. [CrossRef] [PubMed]

Disclaimer/Publisher's Note: The statements, opinions and data contained in all publications are solely those of the individual author(s) and contributor(s) and not of MDPI and/or the editor(s). MDPI and/or the editor(s) disclaim responsibility for any injury to people or property resulting from any ideas, methods, instructions or products referred to in the content.